ELSEVIER

Polymer 41 (2000) 991–1001

polymer

Singlet probes based on coumarin derivatives substituted in position 3; spectral properties in solution and in polymer matrices

M. Kaholek, P. Hrdlovič*, J. Bartoš

Polymer Institute of the Slovak Academy of Sciences, 842 36 Bratislava, Dúbravska cesta 9, Slovak Republic

Received 2 October 1998; received in revised form 16 February 1999; accepted 16 March 1999

Abstract

Spectral properties of coumarin derivatives (2H-1-benzopyran-2-one), substituted with a bulky group in position 3, were investigated in solvents and in polymer matrices. The bulky electron donating groups in position 3 were phenyl-, phenyltio-, 2-methylphenyltio-, 2,6-dimethylphenyltio-, benzyl-, phenoxy-, dimethylamino- and benzoylamino-. The absorption spectra of all the derivatives are dominated by a broad band with a maximum at 340 nm ($\log \varepsilon \sim 4.0$), which were not influenced by the polarity or viscosity of the environment. The fluorescence of these derivatives is strongly influenced by the polarity of the solvent and viscosity of the surroundings. In high viscosity solvents and in polymer matrices, the quantum yields of around 0.1 and a lifetime of around 2 ns was observed. In low viscosity non-polar solvents such as cyclohexane, the quantum yields lower than 0.01 were observed. The fluorescence of coumarin probes was quenched by polar methanol with a bimolecular rate constant, k_q, larger than diffusion controlled limit indicating static quenching. The increased polarity of the mixed solvent introduces processes such as intramolecular charge transfer or twisted intramolecular charge transfer which effectively compete with fluorescence. The dependence of quantum yield of fluorescence on temperature was determined in viscose solvents and polymer matrices. The activation energy of radiation-less process (E_a) increased in going from phenyl to more the bulky 2,6-dimethylphenyltio group in non-polar high viscosity polybutene oil and polar glycerol supporting the idea that the radiation-less process is related to rotation of the group in position 3. The E_a value is lower in rubbery matrices such as polyoctenamer or atactic polypropylene than in glassy polymers such as polystyrene, poly(methyl methacrylate) or polyvinyl chloride. 3-Phenylcoumarin, due to its spectral properties, seems to be the most suitable probe for monitoring microviscosity in polymers.

Keywords: Fluorescence probes; Polymer matrix; 3-Substituted coumarins

1. Introduction

The environment of the molecule determines its basic properties such as solubility or optical properties. Suitable spectroscopic probes can be employed to investigate the microenvironment of macroscopically homogeneous solutions, micelles and polymers, and to correlate changes of photophysical parameters with modification of the structure. Singlet probes exhibiting fluorescence are suitable to monitor the processes occurring in the nanosecond time scale [1–4]. Triplet probes are suitable for longer processes in the micro- and millisecond regions in ordered systems at lower temperatures [5,6]. Aromatic hydrocarbons or dyes are mainly singlet probes preferentially localized in hydrophobic microregions. The exact localization of singlet probes is not always certain. The changes in micropolarity form the basis for the detection of the polymer–dopant interaction. Therefore, suitable probes must exhibit fluorescence sensitive to the environment and can yield information on diffusion, rotation, energy transfer, conformational changes, character of microenvironment, etc. This information can be obtained from polymers or polymers doped with a free or bound fluorescence probe.

Considerable attention has been devoted to the studies of spectral properties of parent coumarin [7] and its derivatives substituted in positions 3–8 [8–12] in order to understand the photophysics of these compounds as laser dyes. A strong dependence of quantum yields and mean fluorescence lifetime on environment has been found for 4-alkyl and 7-alkoxy substituted coumarin derivatives [13]. Moreover, the photophysical behaviour of 3-chloro-4-methyl-7-methoxycoumarine is influence by polarity of the solvent. The internal conversion rate constant (k_{IC}) changes by two orders of magnitude in going from non-polar solvents to polar water. The dramatic variation of k_{IC} is due to the fact that there is a decrease of activation energy of internal conversion (radiation-less process) because the $S_2(n\pi^*)$ state is lying close to $S_1(\pi\pi^*)$. Increasing solvent polarity widens

* Corresponding author.

0032-3861/00/$ - see front matter
PII: S0032-3861(99)00241-4

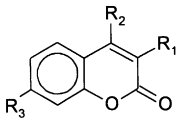

	R_1	R_2	R_3
I	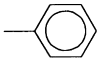	H	H
II	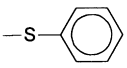	H	H
III	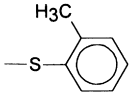	H	H
IV	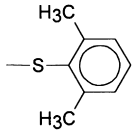	H	H
V	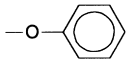	H	H
VI	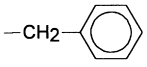	H	H
VII	$-N(CH_3)_2$	H	H
VIII	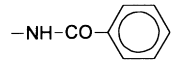	H	H
IX	H	CH_3	$-N(C_2H_5)_2$

Scheme 1. Structure of coumarin derivatives.

the gap between these states and decreases the magnitude of the effect and consequently increases the quantum yield of fluorescence [14].

Recently the dramatic increase in fluorescence intensity (up to seven times) has been observed for 7-diethylamino-4-methylcoumarin (Coumarin 1) in the restricted geometry of a pillared clay nanocomposite [15]. The coumarin and its derivative attract attention as probes to monitor various aspects of the environment.

In this paper we extent our previous study [16] on spectral properties of coumarin derivatives substituted in position 3 with the bulky electron donating substituents in solution and polymer in a broader temperature range. The goal of the study is to obtain more data in order to relate the rotation of the substituent in position 3 with the radiation-less process, on quenching by polar solvents, and on micro-environment (microviscosity, free volume) of polymer matrices. These data can be used for characterization of the probe itself or of its environment.

2. Experimental

2.1. Materials

Coumarin derivatives substituted in position 3, were obtained from the Department of Organic Chemistry, Faculty of Science, Comenius University, Bratislava and several of them were used previously [16]. Their structures, given in Scheme 1, are: 3-phenylcoumarin (**I**), m.p. 135–138°C; 3-phenylthiocoumarin (**II**) m.p. 117–119°C; 3-(2-methylphenylthio)coumarin (**III**), m.p. 143–147°C; 3-(2,6-dimethylphenylthio)coumarin (**IV**), m.p. 167–168°C; 3-phenoxycoumarin (**V**), m.p. 115–116°C; 3-benzylcoumarine (**VI**), m.p. 106–108°C;, 3-dimethylaminocoumarin (**VII**), m.p. 84.5–85.5°C and 3-benzoylaminocoumarin (**VIII**), m.p. 172–174°C. The purity of the coumarin derivatives was controlled by spectroscopy and chromatography (TLC). Laser dye Coumarin 1 (7-diethylamino-4-methylcoumarin, **IX**) was a commercial product (Aldrich, Steinheim, Germany).

Anthracene was zonally refined and quinine sulphate was an analytical reagent (Lachema, Brno, CR). Cyclohexane, methanol and ethanol were for UV spectroscopy (Merck, Darmstadt, Germany), chloroform (Mikrochem Ltd., Bratislava, SR), tetrahydrofurane (BDH, Poole, England) and glycerol (Lachema Ltd., Brno, CR) were analytical reagents. Polybutene oil (Hyvis 10) was a commercial product (BP, Chemicals Ltd., London, England).

Polymer films were prepared by casting from solution or by hot pressing of impregnated polymer powder. Polystyrene (PS, Vestyron, Huls AG, Germany), poly(methyl methacrylate) (PMMA, Diacon, ICI, England), atactic polypropylene (aPP, Slovnaft, Bratislava, SR) and polyoctenamer (VEST, Vestenamer 8012 Huls, Germany) were prepared by casting of polymer solution (chloroform, 5 g/100 ml) on the glass plate (26×38 mm^2). The solvent was allowed to evaporate slowly. Films of polyvinylchlorid (PVC, Neralit, Spolana Neratovice, CR) were cast from tetrahydrofurane solution. All films were self-supporting except for aPP and VEST. Polyoctenamer was purified by precipitation of the toluene solution by methanol and the solution of aPP in ether was precipitated by methanol. The thickness of the films was 50 μm and the dopant concentration was 0.002–0.01 mol kg^{-1}.

Films of polyethylene (PE, Bralen, Slovnaft Bratislava, SR) and isotactic polypropylene (iPP, Daplen, PCD Linz, Austria) were prepared by hot pressing of the powder impregnated by coumarin probes. Polymer powder (2 g), singlet probe (4 mg) and 10 ml of chloroform were mixed and allowed to stand for 24 h. After removal of the solvent and drying, a part of the powder (1 g) was pressed under 0.8 MPa at 140°C for PE and at 190°C for iPP and then

Table 1
Spectral characteristics of coumarin derivatives substituted at position 3 in solution and in polymer matrices

Compound[a]	Medium[b]	λ_a[c] (nm)	log ε[d]	λ_{exc}[e] (nm)	λ_{em}[f] (nm)	$\Delta\tilde{\nu}$[g] (cm^{-1})	Φ_F[h]	τ_F[i] (ns)	$G^{1/2}$[j]
I	Cy	325	4.23	337	399	5 707	0.054		
	EtOH	321	4.17	337	401	6 215	0.087		
	PS	330	3.89	340	403	5 489	0.556	0.56	2.7
	PMMA	325	3.81	335	399	5 707	0.570	0.41	2.6
	PVC	330	4.23	348	401	5 365	1.026	0.61	1.7
II	Cy	334	4.21	347	464	8 388	0.0079		
	EtOH	335	4.08	351	522	10 694	0.0014		
	PS	338	3.94	348	470	8 309	0.227	2.9	4.8
	PMMA	336	3.84	343	467	8 349	0.547	4.3	4.6
	PVC	338	3.90	347	471	8 354	0.407	4.1	6.0
III	Cy	334	4.24	340	456	8 010	0.0032		
	EtOH	335	4.09	351	516	10 471	0.0007		
	PS	339	3.99	349	466	8 039	0.112	2.1	6.1
	PMMA	336	3.86	345	466	8 303	0.314	2.3	6.0
	PVC	338	4.07	345	467	8 173	0.112	3.1	6.6
IV	Cy	335	4.25	330	452	7727	0.0042		
	EtOH	337	4.16				–[k]		
	PS	339	4.02	349	443	6 925	0.314	1.4	2.9
	PMMA	337	3.88	343	436	6 738	0.393	1.7	4.1
	PVC	339	3.92	345	443	6 925	0.673	1.9	4.4
V	Cy	309	3.95	332	377	5 837	0.0065		
	EtOH	310	3.85	328	399	7 195	0.012		
	PS	313	3.63	324	393	6 504	0.040	1.1	5.6
	PMMA	309	3.51	320	387	6 523	0.052	0.57	3.5
	PVC	311	3.60	325	387	6 315	0.244	0.79	3.8
VI	Cy	312	3.76				–[k]		
	EtOH	310	3.85				–[k]		
	PS	314	3.52				–[k]		
	PMMA	312	3.54	330	382	5873	0.0098		
	PVC	314	3.56	330	381	5600	0.023		
VII	Cy	335	4.48	346	454	7 824	0.026		
	EtOH	338	3.97				–[k]		
	PS	342	3.99	351	470	7 963	0.138	1.6	1.5
	PMMA	339	3.85	348	469	8 177	0.180	1.2	2.6
	PVC	343	3.93	350	470	7 878	0.147	1.3	3.4
VIII	Cy	340	4.36	333	367	2 164	0.020		
	EtOH	326	4.31	335	377	4 150	0.0046		
	PS	342	3.97	332	374	2 502	0.741	0.71	2.8
	PMMA	327	4.04	330	372	3 699	0.843	0.7	2.8
	PVC	329	4.03	332	373	3 585	0.992	0.73	2.0
IX	Cy	369	4.34	365	395	1 784	2.81	2.5	1.3
	EtOH	375	4.34	380	449	4 395	1.19	2.9	1.0
	PS	373	4.34	373	413	2 597	3.60	2.8	0.8
	PMMA	368	4.30	373	420	3 364	3.56	3.7	1.4
	PVC	377	4.32	378	426	3 051	3.56	3.5	2.1

[a] Compounds are shown in Scheme 1.
[b] Medium: Cy, cyclohexane; EtOH, ethanol; PS, polystyrene; PMMA, poly(methyl methacrylate); and PVC, polyvinyl chloride.
[c] Wavelength of the absorption band.
[d] Molar decadic extinction coefficient ($dm^3\ mol^{-1}\ cm^{-1}$).
[e] Wavelength of excitation.
[f] Wavelength of fluorescence.
[g] Stoke's shift.
[h] Quantum yield relative to anthracene in the given medium.
[i] Lifetime of the fluorescence determined by the phase plane method.
[j] Standard deviation.
[k] The emission was not measurable.

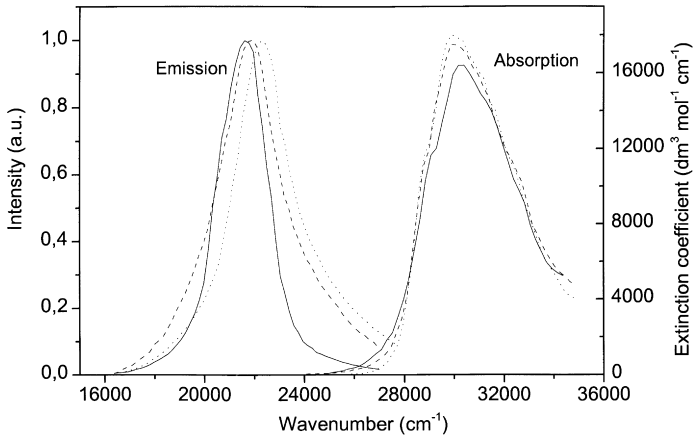

Fig. 1. Fluorescence and long-wavelength absorption spectra of coumarin probes: probe **II** (solid curves), probe **III** (dashed curves) and probe **IV** (dotted curves) in cyclohexane.

rapidly cooled. The thickness of the films was 0.1–0.15 mm and the dopant concentration was 0.01 mol kg^{-1}.

2.2. Instrumentation

The absorption spectra were measured on spectrometer M-40 (C. Zeiss, Jena, Germany). The emission spectra were taken on spectrofluorometer MPF-4 (Perkin–Elmer, Norwalk Co., USA) which was connected through an A/D converter and interfaced to a microcomputer [17]. The emission spectra of the solutions were measured in a right angle arrangement in the cell with controlled temperature. The emission spectra of the polymer films were recorded in a front face arrangement in a solid sample holder at room temperature. For the temperature dependence of the probe fluorescence doped in polymer matrices, the polymer films were placed in a standard thermostated cell (10×10 mm^2) diagonally immersed in water. The quantum yield was determined relative to anthracene in solution and polymer matrix. The quantum yield of anthracene in solution was checked with quinine sulphate. The absolute quantum yields of coumarin derivatives were determined assuming that the anthracene fluorescence is independent of the medium. The quantum yield (Φ_F) was determined according to the relation [18]:

$$\Phi_F = \Phi_F^S \frac{\int_0^\infty I_F(\tilde{\nu})\,d\tilde{\nu}}{\int_0^\infty I_F^S(\tilde{\nu})\,d\tilde{\nu}} \left(\frac{1 - 10^{-A^S}}{1 - 10^{-A}} \right), \quad (1)$$

where Φ_F^S is the quantum yield of anthracene as standard, which was assumed to be 0.25 for all the environments. For the relative quantum yields, the value of Φ_F^S for anthracene was assumed as 1. The integrals $\int_0^\infty I_F(\tilde{\nu})\,d\tilde{\nu}$ and $\int_0^\infty I_F^S(\tilde{\nu})\,d\tilde{\nu}$ are the areas under the emission curves of the investigated compound and standard, A and A^S are the absorbances of the investigated compound and standard at the excitation wavelength. The excitation wavelength was chosen in order to achieve maximum of emission (Table 1). Anthracene was excited at λ_{exc} in the range 356–360 nm depending on the medium.

The decay of emission was measured on the set-up LIF 200 (LTB GmbH, Berlin, Germany) which operates as a stroboscope. Analogous output was digitized in an A/D converter and transferred to a microcomputer [19]. The decay curves were evaluated by the phase plane method [20]. The standard deviation $G^{1/2} = \sum((I_{cal} - I_{exp})^2/n)^{1/2}$ characterized the quality of fitting. A standard deviation, $G^{1/2}$, higher than 5% indicates that a mono-exponential function does not fit the decay satisfactorily.

3. Results and discussion

3.1. Photophysical properties in solution and in polymer matrices

Polymer matrices as supports are widely used in spectroscopy measurements [21–24]. At present, it is well established that low molecular compounds doped in polymer matrices often exhibit different photophysical and photochemical properties as in solutions. The polymer matrix differs from the low molecular solvent in several aspects. Even at the same structure of monomer unit as for low molecular solvent, the polymer matrix exhibits different microviscosity and mobility. It means that the solvation envelope (layer) around the solute by the polymer has got different mobility as that of analogous low molecular solvent.

The polymer matrix influences the excited states and their decay by different interactions:

1. Specific (hydrogen bond) or non-specific interactions (dipole–dipole) might stabilize the excited states.
2. The viscosity of polymer matrix (mainly microviscosity) influences the mobility (rotation) of the whole molecules or parts of it.

Table 2
Calculated values of k_r, τ_F and k_{nr} for derivatives of coumarin substituted at position 3 in various environments (symbols have the same meaning as in Table 1)

Compound	Medium	ε ($dm^3\ mol^{-1}\ cm^{-1}$)	Φ_F[a]	k_r (s^{-1})	τ_F[b] (ns)	k_{nr} (s^{-1})
I	Cy	1.7×10^4	0.014	1.7×10^8	0.082	1.2×10^{10}
	EtOH	1.5×10^4	0.022	1.5×10^8	0.15	6.5×10^9
	PS	7.8×10^3	0.139	7.8×10^7	1.78	4.8×10^8
	PMMA	6.5×10^3	0.143	6.5×10^7	2.2	3.9×10^8
	PVC	1.7×10^4	0.257	1.7×10^8	1.51	4.9×10^8
II	Cy	1.6×10^4	0.002	1.6×10^8	0.013	7.7×10^{10}
	EtOH	1.2×10^4	0.00035	1.2×10^8	0.0029	3.4×10^{11}
	PS	8.7×10^3	0.057	8.7×10^7	0.66	1.4×10^9
	PMMA	6.9×10^3	0.137	6.9×10^7	1.99	4.3×10^8
	PVC	7.9×10^3	0.102	7.9×10^7	1.29	7.0×10^8
III	Cy	1.7×10^4	0.0008	1.7×10^8	0.0047	2.1×10^{11}
	EtOH	1.2×10^4	0.00018	1.2×10^8	0.0015	6.7×10^{11}
	PS	9.7×10^3	0.028	9.7×10^7	0.29	3.4×10^9
	PMMA	7.2×10^3	0.079	7.2×10^7	1.1	8.4×10^8
	PVC	1.2×10^4	0.028	1.2×10^8	0.23	4.2×10^9
IV	Cy	1.8×10^4	0.0011	$1.8x10^8$	0.0061	1.6×10^{11}
	EtOH	1.4×10^4	–[c]	$1.4x10^8$		
	PS	1.0×10^4	0.079	1.0×10^8	0.79	1.2×10^9
	PMMA	7.6×10^3	0.098	7.6×10^7	1.29	7.0×10^8
	PVC	8.3×10^3	0.168	8.3×10^7	2.02	4.1×10^8
V	Cy	8.9×10^3	0.0016	8.9×10^7	0.018	5.5×10^{10}
	EtOH	7.1×10^3	0.003	7.1×10^7	0.042	2.4×10^{10}
	PS	4.3×10^3	0.01	4.3×10^7	0.23	4.3×10^9
	PMMA	3.2×10^3	0.013	3.2×10^7	0.41	2.4×10^9
	PVC	4.0×10^3	0.061	4.0×10^7	1.53	6.1×10^8
VII	Cy	3.0×10^4	0.0065	3.0×10^8	0.022	4.5×10^{10}
	EtOH	9.3×10^3	–[c]	9.3×10^7		
	PS	9.8×10^3	0.035	9.8×10^7	0.36	2.7×10^9
	PMMA	7.1×10^3	0.045	7.1×10^7	0.63	1.5×10^9
	PVC	8.5×10^3	0.037	8.5×10^7	0.44	2.2×10^9
VIII	Cy	2.3×10^4	0.005	2.3×10^8	0.022	4.5×10^{10}
	EtOH	2.0×10^4	0.0012	2.0×10^8	0.006	1.7×10^{11}
	PS	9.3×10^3	0.185	9.3×10^7	1.99	4.1×10^8
	PMMA	1.1×10^4	0.211	1.1×10^8	1.92	4.1×10^8
	PVC	1.1×10^4	0.248	1.1×10^8	2.25	3.3×10^8
IX	Cy	2.2×10^4	0.703	2.2×10^8	3.2	9.3×10^7
	EtOH	2.2×10^4	0.298	2.2×10^8	1.35	5.2×10^8
	PS	2.2×10^4	0.90	2.2×10^8	4.09	2.4×10^7
	PMMA	2.0×10^4	0.89	2.0×10^8	4.45	2.5×10^7
	PVC	2.1×10^4	0.89	2.1×10^8	4.24	2.6×10^7

[a] Calculated from relative quantum yield Φ_F (Table 1) assuming that quantum yield of anthracene in all environments is 0.25.
[b] Lifetime of the fluorescence determined according to relation (2), where the rate constant of radiation process (k_r) was calculated by relation (5).
[c] The emission was not measurable.

3. Aggregation of dopants (solutes) and its solvation is strongly influenced by the solute–solvent interaction.

The main question of the study of the effect of polymer matrix on emission spectra is whether the reorganization of the solvation envelope occurs during the lifetime of the excited state. It means that the solvation envelope can correspond to the different arrangement of electrons or charges than in the ground state [25,26].

The absorption spectra of coumarin derivatives substituted in position 3 by bulky substituent (Scheme 1) show that low molecular mass solvents such as cyclohexane (Fig. 1) or ethanol and polymer matrices such as PS, PMMA and PVC do not effect the broad band without vibrational structure (Table 1) at around 340 nm. The experimental studies and theoretical calculations indicate that the parent coumarin has got the lowest singlet state S_1 of character $n\pi^*$ [7] which results in low fluorescence. Substitution in positions 3–8 leads to switch from $n\pi^*$ to $\pi\pi^*$ and consequently to the higher fluorescence. Probably the $n\pi^*$ character of the lowest singlet state S_1 is preserved for 3-benzyl derivatives (**VI**) because its fluorescence was not measurable in our experimental set up. Other coumarin derivatives (**I**–**V**, **VII**–**IX**) exhibit broad fluorescence without any vibrational structure. The quantum yield of fluorescence strongly depends on the polarity and the viscosity of the environment. A small hypsochromic shift is observed with increasing the size of the substituent in position 3 for probes **II**, **III**

and **IV** in solvents (Fig. 1) as well as in polymer matrices. It indicates that the substitution in position *ortho* of phenylthio group hinders the formation of the ICT state to some extent, especially in polymer matrices.

Recently, it has been shown that fluorescence of several coumarin derivatives substituted in positions 3,6,7,8 [13] strongly depends on the viscosity of the environment. Previous [16] as well as present data show that the quantum yields of fluorescence of coumarin derivatives substituted in position 3 (Scheme 1) are higher in polymer matrices than is low viscosity solvents (Table 1). The lifetime of the excited state (τ_F) is given by

$$\tau_F = \Phi_F/k_r. \tag{2}$$

The theoretical absorption rate coefficient (k_A) expressed by the absorption and emission integral was determined according to the relation [27]:

$$k_A = \frac{8000\pi \ln 10 c n_F^3}{N n_A} \langle \tilde{\nu}_F^{-3} \rangle^{-1} \frac{g_e}{g_g} \int_0^\infty \frac{\varepsilon(\tilde{\nu})\, d\tilde{\nu}}{\tilde{\nu}}, \tag{3}$$

where

$$\langle \tilde{\nu}_F^{-3} \rangle^{-1} = \frac{\int_0^\infty I_F(\tilde{\nu})\, d\tilde{\nu}}{\int_0^\infty \frac{I_F(\tilde{\nu})}{\tilde{\nu}^3}\, d\tilde{\nu}} \tag{4}$$

n_F, n_A are the solvent refraction indices for the wavelengths corresponding to the fluorescence and the absorption band, N is the Avogadro number, c denotes the velocity of light in vacuum, $\varepsilon(\tilde{\nu})$ the molar absorption coefficient, $I_F(\tilde{\nu})$ describes the normalized energy distribution of the fluorescence spectrum, and g_e, g_g are degeneracy coefficients for the excited and the ground state, respectively. If the molecules are in dilute solution in a transparent solvent of negligible optical dispersion, then $n_F = n_A = n$. Eq. (3) allows the calculation of the value of the radiative transition rate coefficient k_A (or the natural lifetime of the excited S_1 state) based on absorption data. The values of k_A obtained should, in general, be equal to k_r, provided that the mirror-symmetry condition is fulfilled, i.e. when the values of the transition moments for absorption and emission are equal ($\vec{M}_{ge} = \vec{M}_{eg}$) and the populations of the vibrational states of S_0 and S_1 are described by the same distribution function. According to Strickler and Berg [28] and Birks and Dyson [27], greater discrepancies between the k_A and k_r values can be explained only by configurational changes of the molecule in the excited state. A useful rough estimate of k_r can be obtained from intensity of the absorption band applying the approximate relationship [10] derived from the exact formula by Strickler and Berg [28]:

$$k_r = 10^4 \varepsilon \tag{5}$$

where ε is the molar decadic extinction coefficient. The rate constant of radiation-less processes, k_{nr}, is the given by:

$$k_{nr} = (1 - \Phi_F)/\tau_F. \tag{6}$$

Analysis of the radiation and radiation-less processes (Table 2) indicates that the substituent in position 3 influences the radiation-less process, which is sensitive to the environment. It is assumed that the substituents in position 3 of coumarin exhibit rotational, twisting or other kinds of reorientation motion through which the electronic energy is transformed to heat what is an actually internal conversion. High viscosity solvents or polymer matrices decrease the amplitude and the frequency of these motions. Consequently, the quantum yield and lifetime of fluorescence is increased (Table 2).

For coumarin derivatives under study with measurable fluorescence in ethanol (**II**, **III**, **VIII** and **IX**) except for **I**, an increase of the Stoke's shift was observed in going from non-polar cyclohexane to polar ethanol (Table 1). Such stabilization in the excited state in polar ethanol might indicate the large intramolecular charge transfer (ICT) or twisted intramolecular charge transfer (TICT). Moreover, a decrease of the quantum yield of fluorescence was observed in going from cyclohexane to ethanol for all the derivatives except **V**, which exhibit an increase in Stoke's shift. There are several processes, which effectively compete with fluorescence such as formation of intramolecular charge transfer state [29], formation of twisted intramolecular charge transfer state [11,30] and changing the planar structure of amino group to a pyramidal one [11]. Large Stoke's shift (about 8000 cm^{-1}) for some derivatives indicates (Table 1) that the fluorescence originates from different state as corresponding to the Frank–Condon transition.

Reorientation of the solvation sphere during the lifetime of the excited state of dopant in glassy polymers (PS, PMMA, PVC) is negligible at temperatures under T_g. Consequently, no red shift of λ_{em} of fluorescence and an increase of Stoke's shift in going from non-polar PS to polar PVC was observed for coumarin probes (Table 1) as might be expected on data in solution. Radiation-less rate constant, k_{nr}, is higher in PS than in PMMA or PVC. Moreover, an increase in the quantum yield of fluorescence is higher in going from ethanol to PVC than from cyclohexane to PS indicating that the PS matrix is less stiff than PVC and PMMA.

3.2. Quenching measurements

Polar solvents quench the emission of most coumarin probes. Since the quencher (polar solvent) is used in high concentration, dynamic and static quenching might operate at the same time. If both static and dynamic quenching occur, the modified Stern–Volmer equation is to be applied [31]:

$$\Phi_0/\Phi = (1 + k_q \tau_F [Q])(1 + K[Q]), \tag{7}$$

where Φ_0 and Φ are the quantum yields of fluorescence without and with the quencher, k_q the bimolecular rate constant, τ_F the fluorescence lifetime without quencher, K

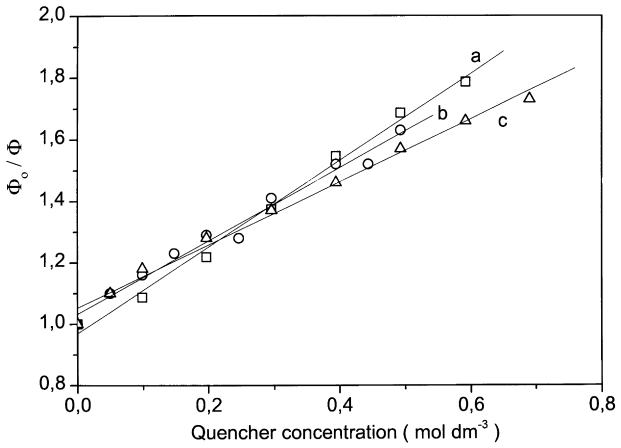

Fig. 2. Stern–Volmer dependence of quenching emission of coumarin probes: (a) probe **II**; (b) probe **III** and (c) probe **IV** with methanol in cyclohexane.

the equilibrium constant for the formation of the dark ground state complex "AQ" and [Q] the quencher concentration. In the absence of static quenching ($K = 0$), the standard Stern–Volmer applies. Addition of methanol to cyclohexane solutions of all coumarin probes except of **I** and **V** decreases their fluorescence and the ratio of Φ_0/Φ on quencher concentration is linear (Fig. 2). The calculated quenching bimolecular rate constants (Table 3), k_q, using estimated values of lifetime, τ_F, are higher than the diffusion controlled bimolecular rate constant in cyclohexane ($k_{diff}^{20} = 0.66 \times 10^{10}$ dm^3 mol^{-1} s^{-1}). Lifetime of the fluorescence (τ_F) was determined according to relation (2), where the rate constant of radiation process (k_r) was calculated using relation (3). Since the estimated lifetimes are very short (Table 3), it is less probable that during the lifetime of the excited state collision occurs. Therefore, static quenching is operating. Molecules of coumarin derivatives are preferentially solvated by methanol forming a "dark complex" AQ which is transformed to the ICT state after excitation. This polar ICT attracts even more polar methanol molecules. At present, we cannot quantify an increase in local concentration of methanol. More polar local environment enriched on methanol induces the transformation of ICT to TICT state [8,30] and its conversion to ground state which is an effective radiation-less route competing with fluorescence. The calculated k_q in this way might be related to reorganization of the solvation sphere of the coumarin probe from ground state to excited ICT or TICT states. Since the actual local concentration of methanol around the coumarin probe is not known, the actual rate of reorganization cannot be determined either. Comparison of K or k_q respectively shows that amino derivatives **VII** and **VIII** are quenched by methanol more effectively than **II**, **III**, and **IV**. This indicates that the amino derivatives have probably more polar ICT (TICT) state than ICT state of **II**, **III**, and **IV**. For Coumarin 1 (**IX**) the quenching bimolecular rate constant is slightly lower than the diffusion controlled one. The fluorescence lifetime of **IX** is substantially longer as compared with other coumarin derivatives. The quenching of **IX** is clearly dynamic although not each collision is effective. Since the estimated lifetimes τ_F are loaded with considerable error, the calculated values of rate constant k_q are approximate as well. Probes **I** and **V** are not quenched by polar methanol because they do not form complexes of ICT or TICT states with polar quencher.

Table 3
Quenching of coumarin probes in cyclohexane by methanol

Compound[a]	τ_F[b] (ns)	K[c] (dm^3 mol^{-1})	$k_q \times 10^{-10}$[d] (dm^3 mol^{-1} s^{-1})
II	0.015	1.4	9.3
III	0.0053	1.2	22.6
IV	0.0066	1.0	15.2
VII	0.019	15.6	82.1
VIII	0.012	19.4	162
IX	2.53[e]	7.5[f]	0.30

[a] Designed according to Scheme 1.
[b] Lifetime of the fluorescence determined according to relation (2), where the rate constant of radiation process (k_r) was calculated by relation (3).
[c] Equilibrium constants for formation of dark complex.
[d] Rate constant for bimolecular quenching.
[e] Lifetime of the fluorescence determined by the phase plane method.
[f] Stern–Volmer constant.

3.3. Temperature effect on radiation-less processes

In order that to gain more insight into the radiation-less processes related to the rotation of the bulky group in position 3 of the parent coumarin, the activation energy (E_a) of this process was determined for coumarin probes in different environments. The fluorescence of several coumarin probes clearly decreased with increasing temperature in high viscosity non-polar mixture polybutene oil Hyvis 10-cyclohexane, 9:1 (Fig. 3) and polar mixture glycerol–ethanol, 9:1 (Fig. 4). Applying Eqs. (2), (5) and (6) and assuming that the absolute quantum yield is substantially lower than 1, the ratio $k_{nr}(T_2)/k_{nr}(T_1)$ can be approximated by $\Phi(T_1)/\Phi(T_2)$. Dependence of $\Phi(T_0)/\Phi(T)$ on $1/T$ yields activation energy (E_a), where T_0 is the lowest temperature of the measurement. In high viscosity solvents, the E_a increases with the size of the group in position 3 starting from phenyl (**I**) and being the largest for 2,6-dimethylphenylthio (**IV**). This fact supports the suggestions that radiation-less processes are related to the motion of this group which moves faster at higher temperature. Higher values of E_a of several probes in mixture Hyvis10–cyclohexane as compared with glycerol–ethanol indicate that the viscosity of Hyvis 10–cyclohexane at 30°C is larger $\eta = 144.23$ P than glycerol–ethanol $\eta = 5.661$ P and consequently, the smaller free volume is available. On the other hand, E_a for Coumarin 1 (**IX**), although it is substantially lower than for other probes, is higher in glycerol–ethanol than in Hyvis 10–cyclohexane. The highly polar excited state of **IX** (ICT or

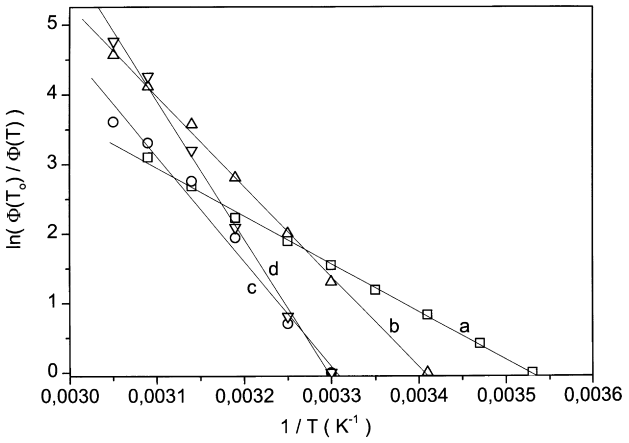

Fig. 3. Dependence of ln(Φ(T_0)/Φ(T)) on 1/T for coumarin probes: (a) probe **I**; (b) probe **II**; (c) probe **III** and (d) probe **IV** in polybutene oil Hyvis 10–cyclohexane mixture (9:1).

TICT) is more tightly solvated in polar solvents because of formation of hydrogen bonds. Surprisingly, Coumarin 1 (**IX**) monitors the same microviscosity in Hyvis10–cyclohexane as in cyclohexane (Table 4). In polar glycerol–ethanol E_a follows the changes of viscosity. The E_a value of probe **VII** was not possible to determine in polar glycerol–ethanol because its fluorescence is completely quenched.

At present, it is generally accepted that the free volume and the size and structure of the molecule or part of it are the decisive factors controlling chemical and physical processes in polymers. Glassy polymers are often considered to be amorphous solids containing sub-microscopic 'holes' with a distribution of sizes defined by the length of a moving polymer segment and a jump frequency. Macroscopic and microscopic polarity, viscosity, glass temperature, tacticity and history of the sample might influence the photophysical and photochemical properties of the doped molecule. Free volume or microviscosity concept is suitable for description of mobility of the doped molecule in the polymer matrix.

Table 4
Activation energy E_a of radiation-less processes for coumarin probes

Compound[a]	Medium[b]	λ_{exc} (nm)	λ_{em} (nm)	E_a (kJ mol^{-1})
I	Gly–EtOH	340	405	33
	Hyvis–Cy	341	398	57
II	Gly–EtOH	364	505	69
	Hyvis–Cy	357	460	108
III	Gly–EtOH		–[c]	
	Hyvis–Cy	361	455	126
IV	Gly–EtOH	367	471	80
	Hyvis–Cy	357	437	165
VII	Gly–EtOH		–[c]	
	Hyvis–Cy	362	454	31
IX	Gly–EtOH	390	462	35
	Hyvis–Cy	367	398	12.5
	EtOH	380	449	14.5
	Cy	365	395	8.5

[a] Designed according to Scheme 1.
[b] Medium: Gly–EtOH mixture glycerol–ethanol 9:1, Hyvis–Cy mixture polybutene oil Hyvis 10–cyclohexane 9:1.
[c] Weak emission for measurements.

Coumarin substituted in position 3 by phenyl group (probe **I**) was used to investigated the mobility of the polymer matrix. This derivative was chosen because it exhibits relatively intense fluorescence, which is strongly dependent on environment, and its excited state is the least polar among the coumarins included in this study. It was found that activation energy (E_a) of the radiation-less process (k_{nr}) is lower in elastomers than in amorphous glassy (Fig. 5) or in semicrystalline polymers (Fig. 6). In our effort to understand the observed facts concerning the radiation-less deactivation of the electronic energy, we try to relate the activation-energy parameters of this radiation-less process with the free volume microstructure characteristics of the matrices investigated. The idea behind this attempt is based on the plausible assumptions that (1) the radiation-less deactivation is associated with the rotation of the phenyl groups and that (2) this rotation process requires a certain

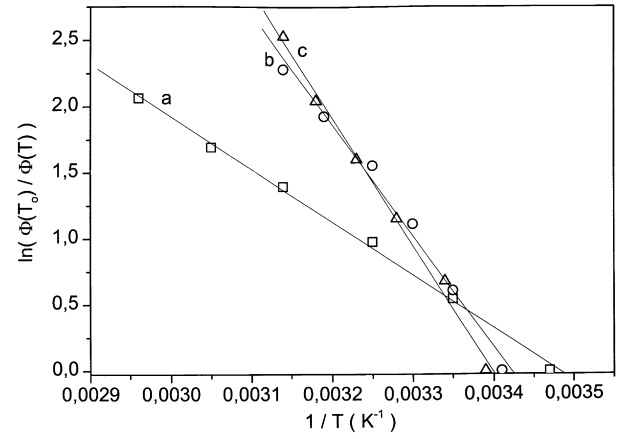

Fig. 4. Dependence of ln(Φ(T_0)/Φ(T)) on 1/T for coumarin probes: (a) probe **I**; (b) probe **II**; (c) probe **IV** in glycerol–ethanol mixture (9:1).

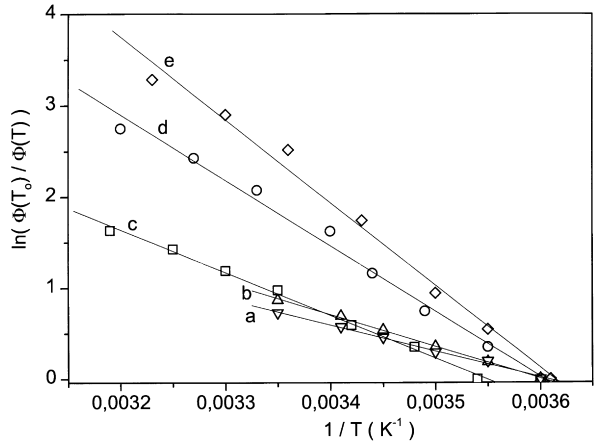

Fig. 5. Dependence of ln(Φ(T_0)/Φ(T)) on 1/T for coumarin probe **I** in polymer matrices: (a) VEST; (b) aPP; (c) PS; (d) PMMA and (e) PVC.

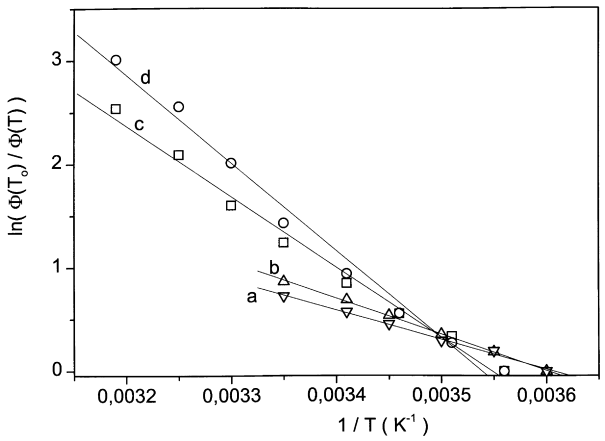

Fig. 6. Dependence of $\ln(\Phi(T_0)/\Phi(T))$ on $1/T$ for coumarin probe **I** in polymer matrices: (a) VEST; (b) aPP; (c) LDPE and (d) iPP.

free space in the vicinity of the moving group. Positron annihilation lifetime spectroscopy (PALS) is a powerful technique to direct detection and measurement of the free volume microstructure in disordered systems [32,33]. The *ortho*-positronium (*o*-Ps), being the bound system of electron and positron, is localized and stabilized for the mean lifetime τ_3 in the local regions of a matrix with the reduced electron density, i.e. free volume holes. The annihilation process of the *o*-Ps in a spherical hole can be described by a simple quantum-mechanical model of the spherical potential well with an electron layer of the thickness ΔR. The semi-empirical relationship between the measured *ortho*-positronium lifetime τ_3 and the free volume hole radius R_h is [34]:

$$\tau_3 = \frac{1}{2}\left[1 - \frac{R_h}{R_0} + \frac{1}{2}\sin\left(2\pi\frac{R_h}{R_0}\right)\right]^{-1}, \quad (8)$$

where $R_0 = R_h + \Delta R$; $\Delta R = 1.656$ Å has been determined from fitting the experimental values of τ_3 obtained for

Table 5
Summarizes the mean *o*-Ps lifetime values at room temperature together with the corresponding free volume hole size characteristics as represented by their hole radius R_h and volume V_h

Polymer[a]	τ_3[b] (ns)	R_h[c] (Å)	V_h[d] (Å^3)	References
aPP	2.35	3.16	132	[35]
PS	2.05	2.9	101	[36]
PMMA	1.94	2.8	93	[37]
PVC	1.81	2.68	81	[38]
LDPE	2.70	3.4	168	[39]
iPP	2.32	3.13	128	[39]

[a] Polymers are designed as given in Section 2.
[b] The mean *ortho*-positronium (*o*-Ps) lifetime at room temperature.
[c] The free volume hole radius.
[d] The mean hole volume calculated from $V_h = (4\pi/3)R_h^3$.

materials with the known hole sizes, e.g. molecular crystals and zeolites. The mean *o*-Ps lifetime values at room temperature as found for thermoplastics from the literature data [35–39] and for aPP from our own PALS measurements together with the corresponding mean free volume hole size characteristics as represented by their hole radius R_h and volume V_h are given in Table 5. The correlation between the effective activation energies of the radiationless deactivation processes (E_a) and the mean hole volumes (V_h) for our series of four amorphous polymer matrices is shown in Fig. 7. The inverse relationship between both the quantities indicates that the phenyl group rotation takes place easier in the matrices with the larger free volume hole entities, because the cooperative motion of the matrix chain segments associated with the displacement of this group requires smaller energy. Clearly, the E_a is decreasing with the increasing free volume (Fig. 7). With increasing free volume, E_a approaches the limiting value. The polarity of the matrix does not influence this radiation-less channel of **I** because the Stock's shift is nearly the same for non-polar and polar solvents and matrices. Dependence of the relative quantum yield on the temperature, employing probe

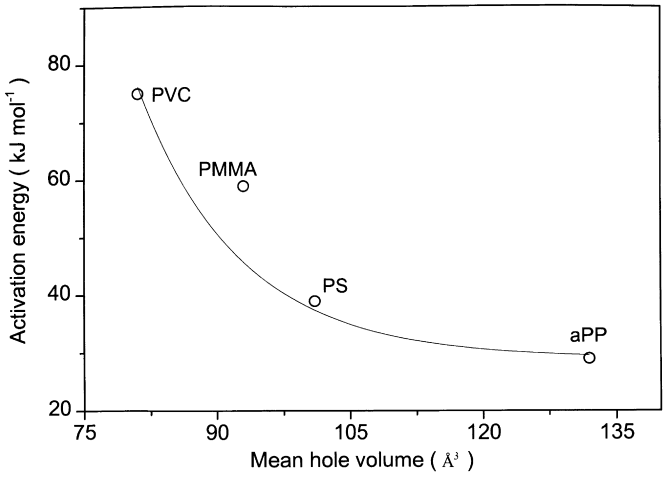

Fig. 7. Dependence of the activation energy E_a of probe **I** on the mean hole volume V_h for several amorphous polymers.

Table 6
Activation energy (E_a) of radiation-less process of probe **I** in different polymer matrices

Polymer[a]	λ_{exc} (nm)	λ_{em} (nm)	V_h[b] (Å^3)	E_a (kJ mol^{-1})
VEST	349	400		24
aPP	347	399	132	29
PS	345	403	101	39
PMMA	345	399	93	59
PVC	349	401	81	75
LDPE	357	400	168	57
iPP	345	398	128	71

[a] Polymers are designed as given in Section 2.
[b] The mean hole volume at respective polymer at room temperature.

I in elastomeric aPP, and VEST were taken up to 25°C because of the leaching of the probe in water. The E_a value of **I** is larger in semicrystalline polymer matrices (LDPE, iPP) than in elastomeric (aPP, VEST) in spite of the fact that the average free volume hole is large or nearly same (Table 6). Doped molecules are located mainly in the amorphous phase and on the interphase of crystalline and amorphous phase. It can be assumed that crystallinity of the polymer and its thermal history might be related to E_a. In the preparation of polymer films of LDPE and iPP by hot pressing and rapid cooling, small crystals are formed [40]. Consequently, there is a larger interphase and less total free volume available. As a result, higher values of E_a for probe **I** are observed for semicrystalline LDPE and iPP than for amorphous aPP and VEST. Films of amorphous polymers were prepared by casting from solution under more or less equilibrated conditions, whereas at hot pressing the conditions are clearly far from equilibrium. The solvation sphere is given by the dopant–polymer interaction (thermodynamic effect) and the preparation process (kinetic effect). The higher E_a for **I** in semicrystalline matrices than in amorphous matrices is caused by the fact that the semicrystalline matrix is formed under conditions which are far from equilibrium which results in a smaller total free volume. In the case of semicrystalline matrices of LDPE and iPP, the presence of the ordered phase acts as a natural hindrance on the cooperative mobility of surrounding chain segments around the moving phenyl group.

Activation energy (E_a) in polymer films is similar to E_a in high viscose polybutene oil Hyvis 10–cyclohexane or glycerol–ethanol mixtures. In fact, the microviscosity of the polymer is several orders of magnitude smaller than as macroscopic viscosity, which for polyethylene corresponds to 10^{10} P. For example, the microviscosity of polyethylene at 80°C is approximately 1 P based on the determination of k_{diff} from quenching of fluorescence of naphthalene [41]. This value is higher as that of mixture glycerol–ethanol (0.12 P) and lower than mixture Hyvis 10–cyclohexane (2.9 P). The changes of E_a for **I** reflects the changes of free volume in polymer matrices. Therefore, 3-phenylcoumarin (**I**) becomes an effective indicator of the microviscosity of the polymer matrices under study. The polarity of matrices does not interfere with this function of **I**.

In conclusion, derivatives of coumarin substituted in position 3 might be applied for the characterization of polymeric matrices generally and 3-phenyl derivative for microviscosity specially.

Acknowledgements

The authors thank the Grant Agency VEGA of the Slovak Republic for financial support through projects 2/4005/97 and 2/4008/97.

References

[1] Kalyanasundaram K. In: Rammamurthy V, editor. Photochemistry in organized and constrained media. New York: VCH Publishers, 1991. Chapter 2.
[2] Kalyanasundaram K, Thomas JK. J Am Chem Soc 1977;99:2039.
[3] Dong DC, Winnik MA. Can J Chem 1984;62:2560.
[4] Winnik FM, Regismond STA. Colloids and Surfaces A 1996;118:1.
[5] Cline-Love LJ, Skrilec M. Analytical Chem 1981;53:1872.
[6] Bolt JD, Turro NJ. Photochem Photobiol 1982;35:305.
[7] Seixas de Melo JS, Becker RS, Macanita AL. J Phys Chem 1994;98:6054.
[8] Arbeloa TL, Arbeloa FL, Tapia MJ, Arbeloa JL. J Phys Chem 1993;97:4704.
[9] Raju BB, Varadarajan TS. J Phys Chem 1994;98:8903.
[10] Raju BB, Varadarajan TS. J Photochem Photobiol A 1995;85:263.
[11] Arbeloa TL, Arbeloa FL, Arbeloa JL. J Luminescence 1996;68:149.
[12] Raju BB, Varadarajan TS. Laser Chem 1995;16:109.
[13] Heldt JR, Heldt J, Ston M, Diehl HA. Spectrochim Acta A 1995;51:1549.
[14] Seixas de Melo JS, Becker RS, Elisei F, Macanita AL. J Chem Phys 1997;107:6062.
[15] Wlodarczyk P, Komarneni S, Roy R, White WB. J Mater Chem 1996;6:1967.
[16] Kaholek M, Hrdlovič P. J Photochem Photobiol A 1997;108:283.
[17] Moyze G, Mlýnek J, Jurčák D, Hrdlovič P. Chem Listy 1992;86:57.
[18] Kawski A, Kubicki A, Kubliňsky B. J Photochem Photobiol A 1993;79:161.
[19] Jurčák D, Mlýnek J, Moyze G, Hrdlovič P. Chem Listy 1989;83:531.
[20] Demas JN, Adamson AW. J Phys Chem 1971;57:2463.
[21] Guillet JE. Polymer photophysics and photochemistry. Cambridge: Cambridge University Press, 1985. Chapter 5.
[22] Michl J, Thulstrup EW. Spectroscopy with polarized light. Solute alignment by photoselection in liquid crystals, polymers and membranes. Deerfield, FA: VCH Publishers, 1986.
[23] Salmassi A, Schnabel W. Polym Photochem 1984;5:215.
[24] Uznanski P, Kryszewski M, Thulstrup EW. Eur Polym J 1991;27:41.
[25] Schmidt E, Loelinger H, Zurcher R. Helv Chim Acta 1978;61:488.
[26] Nadolski B, Uznanski P, Kryszewski M. J Macromol Sci B 1984;23:221.
[27] Birks JB, Dyson DJ. Proc R Soc London A 1963;275:135.
[28] Strickler SJ, Berg RA. J Chem Phys 1962;37:814.
[29] Gáplovský A, Hrdlovič P, Donovalová J, Hrnčiar P. J Photochem Photobiol A 1991;59:221.
[30] Rechthaler K, Köhler G. Chem Phys 1994;189:99.
[31] Fraiji LK, Hayes DM, Werner TC. J Chem Educ 1992;69:424.
[32] Jean YC. Microchem J 1990;42:72.

[33] Bartoš J, Bandžuch P, Šauša O, Krištiaková K, Krištiak J, Kanaya T, Jenninger W. Macromolecules 1997;30:6906.
[34] Nakanishi H, Wang SJ, Jean YC. In: Sharma SC, editor. Positron annihilation studies of fluids. Singapore: World Scientific, 1988.
[35] Bartoš J, Krištiak J. Unpublished results.
[36] Liu J, Deng Q, Jean YC. Macromolecules 1993;26:7149.
[37] Malhotra BD, Pethrick RA. Macromolecules 1983;16:1175.
[38] Jain PC, Bhatnagar S, Gupta A. J Phys C 1972;5:2156.
[39] Uedono A, Kawano T, Tanigawa S, Ban M, Kyoto M, Uozumi T. J Polym Sci B 1997;35:1601.
[40] Wunderlich B. Macromolecular physics: crystal nucleation, growth, annealing, vol. 2. New York: Academic Press, 1976.
[41] Heskins M, Guillet JE. Macromolecules 1970;3:224.